Charge Transfer Plasmons: Optical Frequency Conductances and Tunable Infrared Resonances

Fangfang Wen,[†,∥] Yue Zhang,[‡,∥] Samuel Gottheim,[†,∥] Nicholas S. King,[‡,∥] Yu Zhang,[‡,∥] Peter Nordlander,[‡,§,∥] and Naomi J. Halas*[,†,‡,§,∥]

[†]Department of Chemistry, [‡]Department of Physics and Astronomy, [§]Department of Electrical and Computer Engineering, and [∥]Laboratory for Nanophotonics, Rice University, Houston, Texas 77005, United States

ABSTRACT A charge transfer plasmon (CTP) appears when an optical-frequency conductive pathway between two metallic nanoparticles is established, enabling the transfer of charge between nanoparticles when the plasmon is excited. Here we investigate the properties of the CTP in a nanowire-bridged dimer geometry. Varying the junction geometry controls its conductance, which modifies the resonance energies and scattering intensities of the CTP while also altering the other plasmon modes of the nanostructure. Reducing the junction conductance shifts this resonance to substantially lower energies in the near- and mid-infrared regions of the spectrum. The CTP offers both a high-information probe of optical frequency conductances in nanoscale junctions and a new, unique approach to controllably engineering tunable plasmon modes at infrared wavelengths.

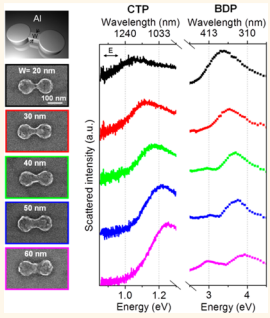

KEYWORDS: charge transfer plasmon · optical antenna · IR plasmon · electric current · single-particle dark-field spectroscopy · electron beam lithography

A nanoscale structure consisting of two metallic nanoparticles separated by a small gap is known as a plasmonic "dimer", which supports hybridized plasmon resonances as a result of the capacitive coupling between the plasmon modes of each nanoparticle.[1−5] For the bonding dipolar dimer plasmon (BDP), this coupling strongly localizes charges at the junction between the two nanoparticles, giving rise to large field enhancements that enable a wide range of applications in surface-enhanced spectroscopy,[6,7] nonlinear optics,[8−10] nanocircuits,[11,12] molecular sensing,[13−16] and optoelectronics.[17,18] If the junction between the two nanoparticles is made conductive, allowing for direct charge transfer from one nanoparticle to the other across the interparticle gap, the plasmons supported by this structure would change profoundly. In this case, the structure will also support an additional, charge transfer plasmon (CTP) at energies lower than the hybridized plasmons supported by the structure. A key distinguishing feature of the CTP is the oscillating electric current through the junction.[19−22] In fact, the appearance of a CTP in the spectrum is a characteristic signature of electron transport at optical frequencies, by quantum tunneling or a classical conductive path, depending on the type of nanostructure.[23−25] The onset of conduction characterized by the appearance of the CTP indicates a drastic modification in both the near and far field properties of the structure, which could have broad applicability in active devices, such as terahertz (THz) frequency photonic devices[26] and ultrafast nanoswitches.[27,28] Theoretical studies have shown that the properties of the CTP depend strongly on junction conductance,[19,29] indicating its potential use as a nonperturbative monitor of optical frequency conductances in nanoscale junctions. This property also provides a systematic route for tuning the CTP frequency in an engineered nanostructure. In previous studies, when the CTP mode appears at substantially lower energies than the other plasmon modes of the structure, it has been studied indirectly, through the modifications it induces in the other plasmon modes of the nanostructure.[21,30] Thus far, direct experimental studies of the CTP have focused primarily on the quantum tunneling

* Address correspondence to halas@rice.edu.

Received for review April 8, 2015 and accepted May 9, 2015.

Published online May 19, 2015
10.1021/acsnano.5b02087

or the optical frequency molecular charge transport regime.[23,31−33] A more comprehensive understanding of CTP properties offers two new advances: (1) the CTP is a unique tool for studying the electron transport of molecules at optical frequencies that are not accessible electronically,[19,33] and (2) the CTP provides a new route to achieving tunable plasmon resonances well into the infrared region of the spectrum.

Here we report a systematic study of the properties of the CTP in individual nanowire-bridged dimer structures, where we control the junction conductance by varying the width, length, and material of the bridging nanowire. We find that small changes of the junction conductance can induce large shifts in the resonance positions and scattering strengths of both the CTP and the BDP modes of the structure. We observe that a dimer bridged by a thin nanowire generates a narrow CTP with a resonance in the near-infrared (NIR) region of the spectrum. By decreasing the nanowire width, the spectral response of the CTP can be tuned into the mid-infrared (MIR) region of the spectrum without a significant broadening, and without significantly increasing the overall dimension of the structure. These highly attractive properties of CTP resonances will be useful for applications in molecular sensing, or as building blocks for new active materials and devices in the MIR region of the spectrum.

RESULTS AND DISCUSSION

A dimer with a conductive bridge can be considered to be the intermediate case between a nonbridged dimer and a nanorod, which can be viewed conceptually as a dimer with a completely filled conductive junction. The calculated scattering efficiencies and charge plots of the plasmon resonances of an Au dimer, an Au dimer connected with a narrow nanowire junction, and an Au nanorod are shown in Figure 1. The diameter of the Au disk is 95 nm, and the thickness of the structures is 35 nm in all cases. The length and width of the junction nanowire are denoted L and W, and are 15 and 30 nm, respectively. The plasmon resonances are calculated for the case where the incident E-field is directed parallel to the dimer axis. For the dimer, the coupling between the two Au disks results in a hybridized BDP mode at ∼1.95 eV (i, blue curve). When the dimer is bridged by a narrow nanowire (red curve), two resonances appear in the spectrum: a blue-shifted BDP at ∼2.1 eV (i, red), and a new low energy resonance at ∼0.96 eV (ii, red). This new narrow resonance can be identified definitively as a CTP from the calculated charge distribution (i in the middle panel of Figure 1b), which indicates an electric current oscillating across the junction at a frequency corresponding to the energy of this mode (Figure S1, Supporting Information). The blue shifting of the BDP, also referred to as the formation of a screened BDP (SBDP), is due to the decreased capacitive coupling

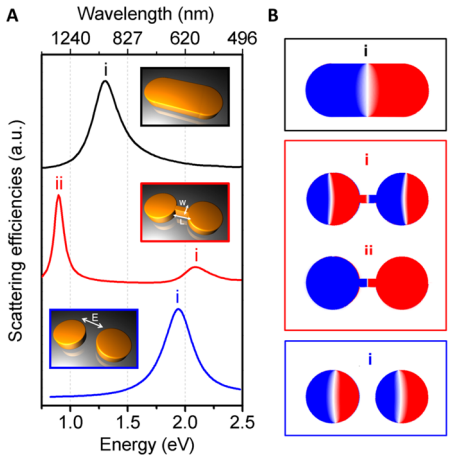

Figure 1. (A) Finite difference time domain (FDTD) calculated scattering efficiencies of a single Au dimer (blue), a nanowire-bridged Au dimer (red), and a Au nanorod (black). The length and the width of the nanowire (red inset) are marked L and W, respectively. The diameter of the disk is 95 nm, the width and the length of junction wire in the junction are 15 and 30 nm, and the thickness of all structures is 35 nm. The E-field direction is oriented along the dimer axis. For the bare dimer, the scattering spectrum shows a BDP resonance at 1.95 eV (i, blue), and a CTP resonance (ii, red) in the NIR at 0.96 eV when the dimer is bridged by a conductive nanowire. A broad resonance appears at 1.3 eV for the nanorod case, when the junction is completely filled (i, black). (B) Charge distributions at the scattering peaks for the structures in (A): a dipolar plasmon for the nanorod, capacitively coupled BDP resonance (i) and charge transfer plasmon (CTP) resonance (ii) for the nanowire-bridged dimer, and a CTP resonance for the dimer.

between the two nanodisks when a conductive medium is present,[19] and to the interaction and hybridization with the lower energy CTP.[34] In the nanorod limit, where the conductive gap is completely filled, the dipolar resonance is red-shifted to ∼1.3 eV. The fundamental difference between the CTP of the nanowire-bridged Au dimer and the dipolar mode of the Au nanorod can be seen by comparing the current density maps of the two structures (Figure S1, Supporting Information), where a prominent oscillating electric current density in the junction of nanowire-bridged Au dimer is observed, while no such feature can be seen in the Au nanorod.

To investigate the CTP and its dependence on junction conductance, we fabricated both Au and Al structures by e-beam lithography, using a scanning electron microscope (FEI QUANTA 650), followed by e-beam evaporation of Au or Al for the different plasmonic structures. For single-particle spectroscopy, Au structures were first patterned in PMMA resist, spin-coated onto a Si substrate coated with a 100 nm oxide layer, followed by e-beam evaporation of a 2 nm Ti adhesion layer and 35 nm of Au. The structures were then obtained by a standard liftoff process in 1-methyl-2-pyrrolidone (NMP). Al nanostructures were fabricated on top of the quartz substrate, evaporated under vacuum at $\sim 2 \times 10^{-7}$ Torr with no adhesion layer, and immersed in acetone for 2 h for liftoff. For ensemble

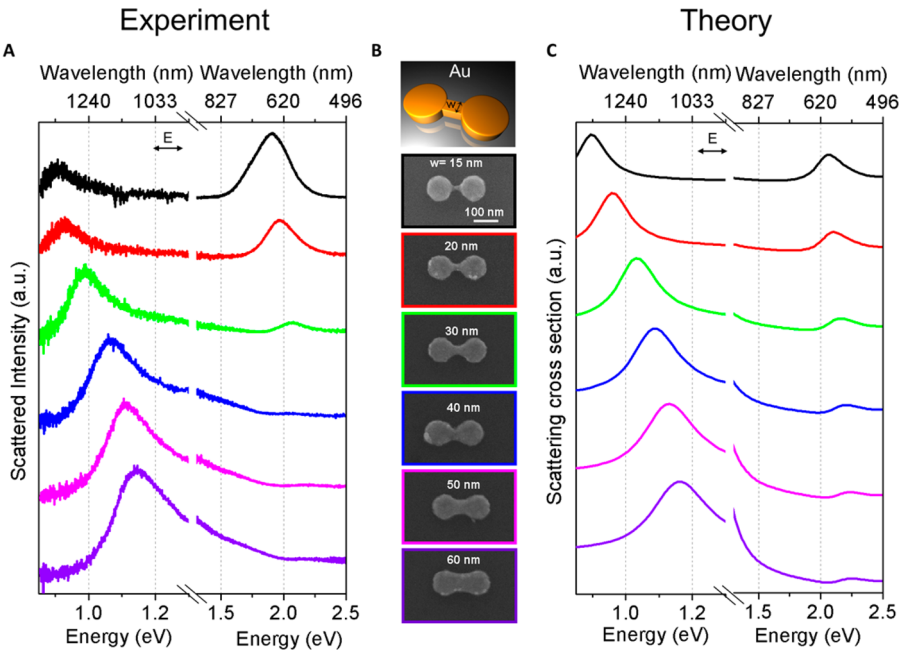

Figure 2. Single-particle dark field scattering properties of nanowire-bridged Au dimers in the visible and NIR regimes. (A) Experimentally measured optical scattering spectra of individual nanowire-bridged Au dimers with a nanowire width increasing from 15 to 60 nm. The diameter of the disk and the length of the wire are kept constant at 95 and 30 nm, and the width of the wire is increased from 15 nm (black) to 60 nm (violet). (B) Schematic representation and SEM images corresponding to the spectra in (A) of the bridged Au dimer structures. (C) FDTD calculations of the scattering spectra of the structures shown in (B) in the NIR and visible regimes, respectively.

optical measurements, all structures were fabricated on a quartz substrate for transmission measurements using a commercial Fourier transform infrared spectroscopy (FTIR). The optical response of individual nanostructures was studied by single-particle dark-field scattering spectroscopy using a commercial Zeiss microscope equipped with spectrographs and CCD detectors for obtaining the spectrum of each nanostructure over an extended spectral range.

Scattering spectra of individual nanowire-bridged Au dimers in the visible (500−950 nm, 1.3−2.5 eV) and NIR regime (955−1450 nm, 0.85−1.3 eV), along with the SEM images of the specific nanostructures measured, are shown in Figure 2. For each nanostructure, the spectra were collected in the two relevant wavelength regimes using both visible and near-infrared wavelength CCD detectors. The diameter of the disks is 95 nm, and the thickness of the structure is 35 nm. The length of the Au nanowire in the junction is kept constant at 30 nm, while the width is increased from 15 to 60 nm, and the corresponding optical responses in the visible and NIR were recorded. For each nanostructure, two resonances are clearly observable in the spectrum, with the lower energy feature corresponding to the CTP and the higher energy feature corresponding to the dipolar plasmon mode. For a dimer with a 15 nm-width junction nanowire (black), the NIR CTP plasmon mode appears at 0.9 eV, and is accompanied by a visible dipolar resonance at 1.9 eV. When the width of the nanowire is increased further, the junction conductance is increased, and both the CTP and dipolar dimer plasmon exhibit a gradual shift to higher energies. The amplitude of the resonances also shows a significant dependence on nanowire width, where the strength of the CTP progressively increases with increasing nanowire width, while the amplitude of the dipolar mode is concurrently reduced. When the nanowire width is increased further, to 60 nm (violet), the CTP blue-shifts to ∼1.15 eV and the dipolar mode shifts to 2.2 eV but is now strongly damped. Single-particle FDTD calculations of the scattering properties of each structure, using the equivalent experimental dark-field geometries, were performed (Figure 2C). The simulation results agree quite well with the resonance energies and scattering intensities observed in the experimental measurements, both following the same trends with junction nanowire width. For a 15 nm-width junction nanowire (black curve), the CTP and BDP possess line widths of 0.094 and 0.333 eV, respectively, corresponding well to the predicted narrower line width of the CTP in Figure 1 (red curve). However, with the increase in nanowire width and the concurrent blue-shift of the CTP to higher energies, the line width of the CTP becomes broader as a result of the increased radiation damping (Figure S3, Supporting Information).

We also studied the plasmonic properties of this same series of structures fabricated in aluminum, which we expect to exhibit different CTP and dipolar plasmon resonances. Aluminum as a plasmonic medium

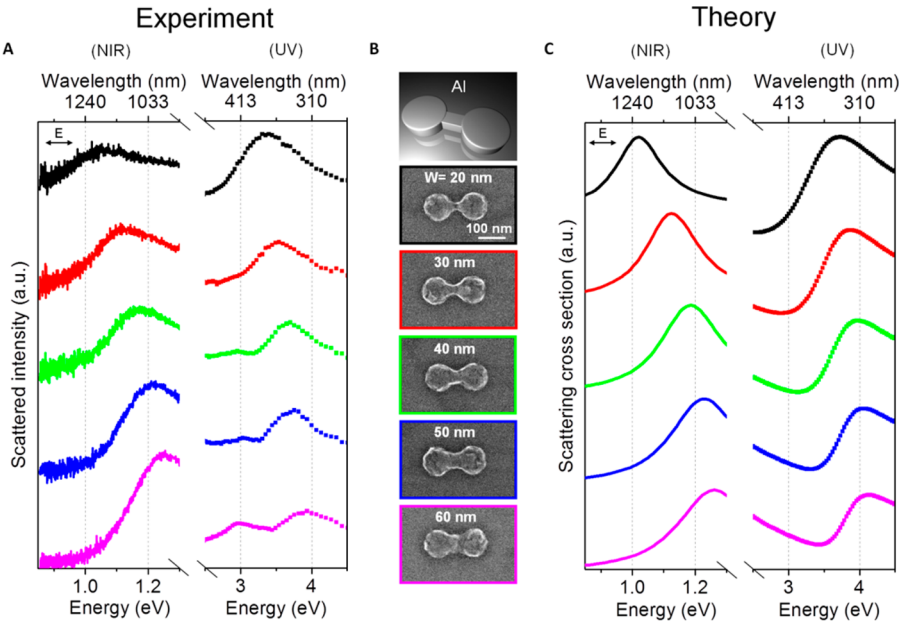

Figure 3. (A) Experimental single-particle dark field scattering spectra of nanowire-bridged Al dimers in the NIR and UV regimes. (B) Schematic and SEM images of each structure. (C) Corresponding FDTD simulations for each structure.

has attracted increasing interest due to its low cost and ready manufacturability along with its optical response in the visible and the UV regime, enabling a wide range of potential applications.[35] According to the tabulated dielectric functions of the two metals, Al has a larger AC conductivity than Au at wavelengths above 500 nm (Figure S4, Supporting Information) and a higher electron density. It is predicted that for the same size and geometry, an Al nanowire-bridged dimer should show a higher CTP energy than an Au nanowire-bridged dimer. Here we perform similar experiments on Al using the same geometries, and capture their optical responses in both the UV and NIR regimes (Figure 3a). SEM images of the nanostructures are shown in Figure 3b. Despite the UV dipolar plasmon resonance of the Al dimer, bridging two Al disks with a nanowire still generates a new CTP in the near-infrared region of the spectrum. The CTP shifts continuously to higher energies, from 1.06 to 1.25 eV, when the nanowire width is increased from 20 nm (black) to 60 nm (magenta). Unlike the Au case, the dipolar plasmon is less damped in the Al structures, and is detectable for all Al dimers using a custom-built UV dark-field microscope. The UV dipolar plasmon also exhibits a blue-shift with increasing junction conductance as well, shifting from 3.4 eV for a 20 nm nanowire width to 3.95 eV for a 60 nm nanowire width. The amplitude of the CTP resonance is enhanced as the junction conductance is increased, while the strength of the dipolar plasmon mode is reduced. These results are reproduced well in a series of FDTD simulations (Figure 3c), where a 4 nm oxide layer is assumed to cover the Al structure.[35]

To better understand the influence of the junction conductance on the CTP, we calculated the junction conductance of each structure at CTP resonances in Au and Al (Figures 2 and 3) and plotted the CTP energy as a function of junction conductance (Figure 4). The conductance is calculated as $G = \sigma(\omega)WH/L$, where $\sigma(\omega)$ is the frequency dependent AC conductivity of the bridging wire and W, H, and L are the width, height, and length of the bridging nanowire. The value of the conductance is expressed as $G = nG_0$, where G_0 is the unit quantum conductance with a value of 77.5 μS. The theoretical (solid squares) and experimental (empty triangles) conductances are determined using the CTP frequency from FDTD simulations and from the experimentally measured CTP resonances, respectively. We see that the experimentally obtained conductances match well with the theoretical values. In Figure 4A, the junction conductance shows a continuous increase with increasing wire width for both Au (black) and Al (red) dimers but exhibits a much larger increase for the Al structures. In general, for structures with the same dimension of the bridging nanowire, Al structures possess a higher junction conductance than Au structures. Unexpectedly, despite a substantially larger conductance at fixed wire width (up to 6 times larger), the CTP energy for Al structures is only slightly higher than for Au structures and requires a larger change of conductance for tuning. To investigate this further, we plotted the CTP as a function of junction conductance over a broad conductance range (Figure 4B). The smaller conductance data points were obtained by performing FDTD simulations of structures with narrower nanowire widths than could be achievable by our current fabrication approach (2, 5, 10 nm, *etc*). In addition, we also calculated the conductances in mixed-metal, Au nanowire-bridged Al dimers

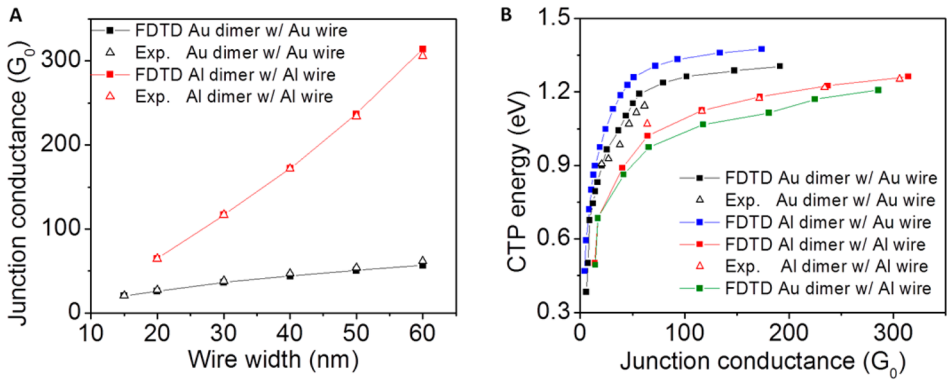

Figure 4. Junction conductance dependence of CTPs in wire bridged Au (Figure 2) and Al dimers (Figure 3). (A) Junction conductances of nanowire bridged dimers at CTP resonances with varying wire widths in Au (black) and Al (red) structures. The solid squares and empty triangles correspond to the conductances calculated from FDTD simulations of the CTP frequency and from experimentally measured CTP frequencies, respectively. (B) CTP resonance as a function of the junction conductance for wire bridged dimers with varying junction materials.

(blue solid squares) and Al nanowire-bridged Au dimers (green solid squares) for the same range of nanowire widths. In all cases, we see that the CTP shows a very high sensitivity to the junction conductance in the small conductance limit, but becomes markedly less sensitive as the conductance increases beyond $50G_0$. Since the junction conductances of our experimentally fabricated Al nanowire-bridged Al dimer, shown in Figure 3, fall into the large conductance regime, the CTP for these structures is relatively insensitive to the junction conductance, resulting in a limited CTP tunability for these structures. For both Au and Al structures, the experimental data (empty triangles) match well with the theoretically obtained trends for these structures (solid squares).

For nanowire-bridged dimers of the same dimension, the CTP frequency depends primarily on the material of the junction nanowire, and less on the disk material. In both Au nanowire-bridged dimers (black and blue solid squares) and Al nanowire-bridged dimers (red and green solid squares), despite the very different plasmon wavelengths of the unlinked Au and Al dimers, bridging them with a nanowire of the same material results in a very similar dependence of the CTP energy on junction conductance. Conversely, for the same dimer bridged with a nanowire of either Au or Al with the same junction conductance (obtained by manipulating the nanowire geometry), the resulting CTP resonances can be quite different. As an example, comparing an Au nanowire-bridged Au dimer (black solid squares) to an Al nanowire-bridged Au dimer (green solid squares) with the same conductance of $45G_0$, the CTP resonances occur at energies of 1.1 and 0.85 eV, respectively.

We also investigated how the BDP energies depend on junction conductances (Figure S6, Supporting Information). Increasing the nanowire width increases the junction conductance, which results in a blueshift of the BDP. Since the values of the conductance are comparable for Au and Al structures, the dipolar plasmon shows a similar sensitivity to the junction conductance in both cases. The blueshift of the BDP with increasing junction wire width and thus junction conductances is further examined in near field plots (Figure S7, Supporting Information). With increasing wire width, the E-field is progressively expelled from the gap, resulting in a successively weaker coupling of the two disks. As a result, the screened dipolar plasmon exhibits a blue shift.[19]

The CTP can be tuned from the NIR to the MIR regime quite simply, by increasing the junction wire length while keeping the nanowire width narrow and thus reducing the junction conductance. SEM images of bridged Au dimers with an increasing wire length from 30 to 90 nm are shown in Figure 5A. The diameter of the disk and the width of the wire are 200 and 20 nm, respectively, and the interstructure distance is 1 μm. The optical response of these structures is collected from arrays of the fabricated structure, using an FTIR in transmission mode. A typical SEM image of the arrays is shown in Figure S8 in the Supporting Information.

We measured the transmitted signal from the arrays and retrieved the absorbance data for each geometry. All spectra were normalized (Figure 5B). The spectra are plotted from 0.3 to 0.8 eV (1.55 to 4.13 μm). A prominent MIR CTP resonance is observed for each geometry, showing a continuous red shift to lower energies from 0.62 to 0.45 eV (1.95 to 2.75 μm) when the length of the junction wire is increased from 30 to 90 nm. An increase of the junction nanowire length increases the charge transport time, giving rise to a lower CTP resonance energy of the structure.[19] This result is reproduced well in a series of FDTD simulations, using perioidic boundary conditions (Figure 5C), confirming that the MIR resonance of these structures can be tuned by varying the junction conductance. We also compared the simulated spectra using periodic boundary condition to the calculated single-particle absorption spectra in Figure S9 in the Supporting Information, where the results show a fairly good

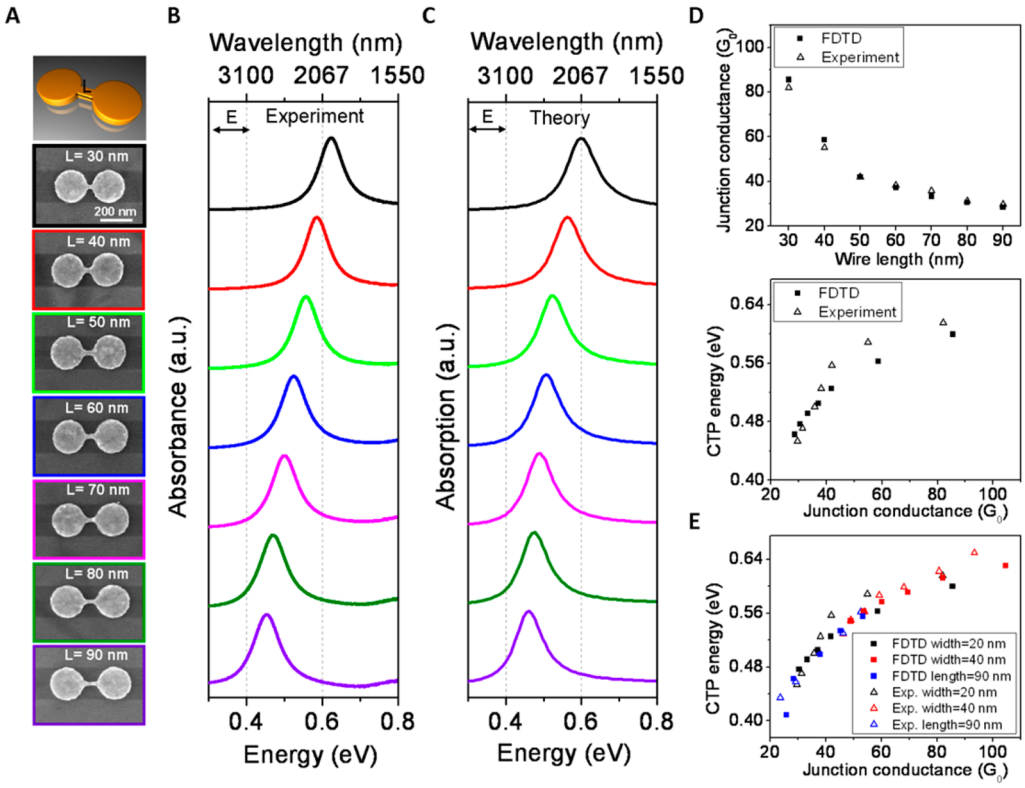

Figure 5. MIR charge transfer plasmons. (A) Schematic and SEM images of the Au dimers bridged by a 20 nm-width gold nanowire with varying wire lengths. (B) FTIR absorbance spectra of dimers with increasing wire lengths from 30 to 90 nm. (C) The corresponding FDTD simulated spectra. (D) The junction conductances at CTP resonances (top) and the CTP energy as a function of junction conductance (bottom). Increasing the wire length (with fixed wire width) reduces the junction conductance and concurrently red-shifts the CTP to the low energy. (E) CTP as a function of junction conductance obtained at various wire widths and lengths.

agreement between the two, indicating minimal far field interference and imhomogeneous broadening effects for the array geometry.

The junction conductances for nanowire-bridged MIR-resonant structures with different nanowire lengths, and their CTP resonance dependence on the junction conductance, are shown in Figure 5D, where experimental data (empty triangles) show a qualitive agreement with FDTD simulations (solid squares). For a fixed nanowire width, the junction conductance is inversely proportional to nanowire length. We performed similar experiments by fixing the nanowire width at 40 nm and varying the nanowire length (Figure S10, Supporting Information), and fixing the nanowire length at 90 nm while increasing the nanowire width (Figure S11, Supporting Information). In each case, the junction conductance was calculated (Figure S12) and the corresponding CTP energy was plotted in Figure 5E. Both the experimental and theoretical data follow the same trend. This indicates that the junction conductance, controlled by the junction geometry, is the only determining factor for the resonance position of the CTP in this regime. In other words, the CTP mode energy would be the same for structures with the same junction conductance, even if their dimensions slightly differ for this geometry. This simple dependence of the CTP resonance on junction conductance provides a direct strategy for the design of nanostructures with specific MIR response. The junction conductance for a desired plasmon resonance can be directly read out from the plot, offering an effective way to engineer a plasmonic system with specifically desired infrared resonant properties. Similar results were also obtained for Al structures, where a MIR CTP can also be observed for nanowire-bridged dimer geometries, also exhibiting a similar tunability of IR resonance with junction conductance (Figure S13, Supporting Information).

As an additional example of CTP tunability, we examine the case of changing the diameter of the disks while keeping the junction wire dimensions constant. Figure 6A shows the CTP dependence of three nanowire-bridged dimer structures with 200, 250, and 300 nm disk diameters, each bridged by a nanowire with a 20 nm width and a 90 nm length. The collected absorbance spectra are shown in Figure 6B, where the CTP peak exhibits a red shift from 0.455 eV (2.73 μm wavelength) to 0.37 eV (3.35 μm wavelength) with increasing disk diameter. The red shift of the CTP resonance can be interpreted in terms of the charge transport time, which is also closely related to the dimer disk diameter. An increase in disk diameter increases the charge separation distance, resulting in a longer

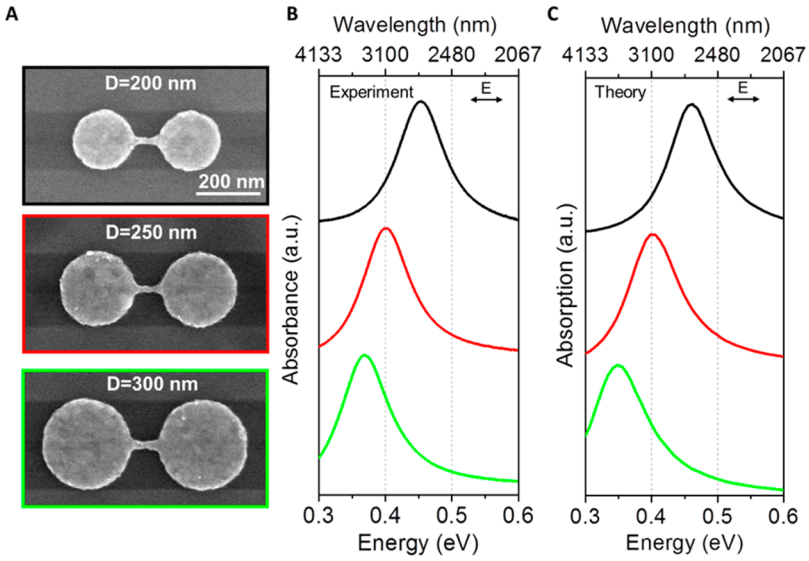

Figure 6. Tuning MIR charge transfer plamons by varying the disk diameter. (A) SEM images of Au dimers of varying diameter bridged by a 20 nm-width and 90 nm-length gold nanowire. (B) FTIR absorbance spectra of antennas with increasing disk diameters from 200 to 300 nm. (C) The corresponding FDTD simulation spectra.

charge transport time, lowering the CTP energy.[19] The CTP tunability observed experimentally is reproduced well by the FDTD simulations in Figure 6C. Similar results can also be found for Al structures (Figure S14, Supporting Information).

CONCLUSIONS

In conclusion, we have performed a comprehensive experimental and theoretical study of the optical properties of nanowire-bridged plasmonic disk dimers. These structures are found to exhibit both standard hybridized resonances due to the capacitive coupling of the disks and pronounced CTP resonances due to the conductive coupling. The energy, intensity, and line width of the CTP resonances are found to be strongly dependent on the junction conductance which can alter simply by changing its geometry or material composition. We explicitly demonstrate this plasmon tunability from the visible into the mid-IR. We find that when tuned into the mid-infrared region of the spectrum the CTP resonance has a narrow line width, an important property to be exploited in future applications. Our results offer an optical platform for measuring the electron transport properties of molecules or nanomaterials at optical frequencies, and provide a strategy for engineering near- and mid-IR plasmonic substrates for surface enhanced IR spectroscopic and sensing applications.

METHODS

Structure Fabrication. Au and Al nanostructures were fabricated by e-beam lithography. For single-particle spectroscopy, Au structures were first defined in PMMA resist spin-coated onto a Si substrate coated with a 100 nm oxide layer, followed by e-beam evaporation of a 2 nm Ti adhesion layer and 35 nm of Au. The structures were then obtained by performing a standard liftoff process in 1-methyl-2-pyrrolidone (NMP). Al nanostructures were fabricated on top of the quartz substrate, evaporated a 35 nm Al layer under a vacuum of $\sim 2 \times 10^{-7}$ Torr with no adhesion layer, and immersed in acetone for 2 h for liftoff. For ensemble optical measurements, Au and Al structures were fabricated on a quartz substrate.

Single Particle Dark-Field Spectroscopy. The optical response of individual nanostructures was studied by single-particle dark-field scattering spectroscopy. Individual Au nanostructures were studied by a commercial Zeiss microscope equipped with visible/NIR spectrographs and CCD detectors, obtaining the spectrum of each nanostructure over the extended range. The UV response of individual Al nanostructures was measured by a home-built UV darkfield microscope. A narrow wavelength band from the light source (Energetiq LDLS) was selected by the monochromator and directed to the sample surface with a 50° incident angle. The scattered signal was collected by a 15× objective with a NA of 0.28 (Edmund Optics, UV ReflX) and detected by a UV-enhanced CCD array (Princeton Instruments). The scattering spectrum was obtained by collecting the signals from 200 to 700 nm excitations with 5 nm increments. All the measurements were performed in a dry N_2 environment.

Fourier Transform Infrared Spectroscopy (FTIR). The optical absorbance spectra of the Au and Al nanostructure arrays were measured using FTIR spectroscopy with a Bruker Vertex 80v spectrometer equipped with a Hyperion 3000 microscope (mercury cadmium telluride detector). The polarization dependent measurements were performed by placing a zinc selenide linear polarizer in the excitation pathway.

Numerical Simulations. The scattering spectra, charge distributions and current density maps were simulated by finite difference time domain method (FDTD, Lumerical Solutions). A plane wave with E-field linearly polarized along the plasmonic dimer axis was employed to analyze the far field and near field properties of the structures.

Conflict of Interest: The authors declare no competing financial interest.

Supporting Information Available: Current density maps of the nanowire-bridged Au dimer and the nanorod; line widths of the structures; summarized CTP and BDP resonance positions; AC conductivity of Au and Al; junction conductances

at the BDP resonances; near field distributions of the Au structures with an increasing wire width at the BDP and CTP resonances; scanning electron microscope image of the ensemble gold structures; absorbance spectra of arrays of Al nanostructures. The Supporting Information is available free of charge on the ACS Publications website at DOI: 10.1021/acsnano.5b02087.

Acknowledgment. We thank Yumin Wang and Bob Zheng for discussions. This work was financially supported by the Robert A. Welch Foundation under Grants C-1220 (N.J.H) and C-1222 (P.N.), the National Security Science and Engineering Faculty Fellowship (NSSEFF) N00244-09-1-0067, the Defense Threat Reduction Agency (DTRA) HDTRA1-11-1-0040, the Air Force Office of Scientific Research (AFOSR) FA9550-10-1-0469, and the Army (MURI W911NF-12-1-0407).

REFERENCES AND NOTES

1. Su, K.-H.; Wei, Q.-H.; Zhang, X.; Mock, J. J.; Smith, D. R.; Schultz, S. Interparticle Coupling Effects on Plasmon Resonances of Nanogold Particles. *Nano Lett.* **2003**, *3*, 1087–1090.
2. Prodan, E.; Radloff, C.; Halas, N. J.; Nordlander, P. A Hybridization Model for the Plasmon Response of Complex Nanostructures. *Science* **2003**, *302*, 419–422.
3. Nordlander, P.; Oubre, C.; Prodan, E.; Li, K.; Stockman, M. I. Plasmon Hybridization in Nanoparticle Dimers. *Nano Lett.* **2004**, *4*, 899–903.
4. Tabor, C.; Van Haute, D.; El-Sayed, M. a. Effect of Orientation on Plasmonic Coupling between Gold Nanorods. *ACS Nano* **2009**, *3*, 3670–3678.
5. Funston, A. M.; Novo, C.; Davis, T. J.; Mulvaney, P. Plasmon Coupling of Gold Nanorods at Short Distances and in Different Geometries. *Nano Lett.* **2009**, *9*, 1651–1658.
6. Ye, J.; Wen, F.; Sobhani, H.; Lassiter, J. B.; Van Dorpe, P.; Nordlander, P.; Halas, N. J. Plasmonic Nanoclusters: Near Field Properties of the Fano Resonance Interrogated with SERS. *Nano Lett.* **2012**, *12*, 1660–1667.
7. Brown, L. V.; Zhao, K.; King, N.; Sobhani, H.; Nordlander, P.; Halas, N. J. Surface-Enhanced Infrared Absorption Using Individual Cross Antennas Tailored to Chemical Moieties. *J. Am. Chem. Soc.* **2013**, *135*, 3688–3695.
8. Zhang, Y.; Wen, F.; Zhen, Y.-R.; Nordlander, P.; Halas, N. J. Coherent Fano Resonances in a Plasmonic Nanocluster Enhance Optical Four-Wave Mixing. *Proc. Natl. Acad. Sci. U.S.A.* **2013**, *110*, 9215–9219.
9. Aouani, H.; Rahmani, M.; Navarro-Cía, M.; Maier, S. A. Third-Harmonic-Upconversion Enhancement from a Single Semiconductor Nanoparticle Coupled to a Plasmonic Antenna. *Nat. Nanotechnol.* **2014**, *9*, 290–294.
10. Wang, Y.; Abb, M.; Boden, S. a.; Aizpurua, J.; De Groot, C. H.; Muskens, O. L. Ultrafast Nonlinear Control of Progressively Loaded, Single Plasmonic Nanoantennas Fabricated Using Helium Ion Milling. *Nano Lett.* **2013**, *13*, 5647–5653.
11. Engheta, N. Circuits with Light at Nanoscales: Optical Nanocircuits Inspired by Metamaterials. *Science* **2007**, *317*, 1698–1702.
12. Liu, N.; Wen, F.; Zhao, Y.; Wang, Y.; Nordlander, P.; Halas, N. J.; Alu, A. Individual Nanoantennas Loaded with Three-Dimensional Optical Nanocircuits. *Nano Lett.* **2013**, *13*, 142–147.
13. Camden, J. P.; Dieringer, J. a; Wang, Y.; Masiello, D. J.; Marks, L. D.; Schatz, G. C.; Van Duyne, R. P. Probing the Structure of Single-Molecule Surface-Enhanced Raman Scattering Hot Spots. *J. Am. Chem. Soc.* **2008**, *130*, 12616–12617.
14. Ahmed, A.; Gordon, R. Single Molecule Directivity Enhanced Raman Scattering Using Nanoantennas. *Nano Lett.* **2012**, *12*, 2625–2630.
15. Liu, N.; Tang, M. L.; Hentschel, M.; Giessen, H.; Alivisatos, a P. Nanoantenna-Enhanced Gas Sensing in a Single Tailored Nanofocus. *Nat. Mater.* **2011**, *10*, 631–636.
16. Shegai, T.; Johansson, P.; Langhammer, C.; Käll, M. Directional Scattering and Hydrogen Sensing by Bimetallic Pd-Au Nanoantennas. *Nano Lett.* **2012**, *12*, 2464–2469.
17. Knight, M. W.; Sobhani, H.; Nordlander, P.; Halas, N. J. Photodetection with Active Optical Antennas. *Science* **2011**, *332*, 702–704.
18. Mubeen, S.; Hernandez-Sosa, G.; Moses, D.; Lee, J.; Moskovits, M. Plasmonic Photosensitization of a Wide Band Gap Semiconductor: Converting Plasmons to Charge Carriers. *Nano Lett.* **2011**, *11*, 5548–5552.
19. Pérez-González, O.; Zabala, N.; Borisov, a. G.; Halas, N. J.; Nordlander, P.; Aizpurua, J. Optical Spectroscopy of Conductive Junctions in Plasmonic Cavities. *Nano Lett.* **2010**, *10*, 3090–3095.
20. Fontana, J.; Ratna, B. R. Highly Tunable Gold Nanorod Dimer Resonances Mediated through Conductive Junctions. *Appl. Phys. Lett.* **2014**, *105*, 011107.
21. Sun, Y.; Foley, J. J.; Peng, S.; Li, Z.; Gray, S. K. Interfaced Metal Heterodimers in the Quantum Size Regime. *Nano Lett.* **2013**, *13*, 3958–3964.
22. Schnell, M.; García-Etxarri, a.; Huber, a. J.; Crozier, K.; Aizpurua, J.; Hillenbrand, R. Controlling the Near-Field Oscillations of Loaded Plasmonic Nanoantennas. *Nat. Photonics* **2009**, *3*, 287–291.
23. Savage, K. J.; Hawkeye, M. M.; Esteban, R.; Borisov, A. G.; Aizpurua, J.; Baumberg, J. J. Revealing the Quantum Regime in Tunnelling Plasmonics. *Nature* **2012**, *491*, 574–577.
24. Scholl, J. A.; Garc, A.; Koh, A. L.; Dionne, J. A. Observation of Quantum Tunneling between Two Plasmonic Nanoparticles. *Nano Lett.* **2013**, *12*, 564–569.
25. Wiener, A.; Duan, H.; Bosman, M.; Horsfield, A. P.; Pendry, J. B.; Yang, J. K. W.; Maier, S. A.; Ferna, A. I. Electron-Energy Loss Study of Nonlocal Effects in Connected Plasmonic Nanoprisms. *Nano Lett.* **2013**, 6287–6296.
26. Gu, J.; Singh, R.; Liu, X.; Zhang, X.; Ma, Y.; Zhang, S.; Maier, S. a; Tian, Z.; Azad, A. K.; Chen, H.-T.; et al. Active Control of Electromagnetically Induced Transparency Analogue in Terahertz Metamaterials. *Nat. Commun.* **2012**, *3*, 1151.
27. Large, N.; Abb, M.; Aizpurua, J.; Muskens, O. L. Photoconductively Loaded Plasmonic Nanoantenna as Building Block for Ultracompact Optical Switches. *Nano Lett.* **2010**, *10*, 1741–1746.
28. Abb, M.; Albella, P.; Aizpurua, J.; Muskens, O. L. All-Optical Control of a Single Plasmonic Nanoantenna-ITO Hybrid. *Nano Lett.* **2011**, *11*, 2457–2463.
29. Fontana, J.; Ratna, B. R. Highly Tunable Gold Nanorod Dimer Resonances Mediated through Conductive Junctions. *Appl. Phys. Lett.* **2014**, *105*, 011107.
30. Atay, T.; Song, J. H.; Nurmikko, A. V. Strongly Interacting Plasmon Nanoparticle Pairs: From Dipole-Dipole Interaction to Conductively Coupled Regime. *Nano Lett.* **2004**, *4*, 1627–1631.
31. Duan, H.; Fernández-Domínguez, A. I.; Bosman, M.; Maier, S. a; Yang, J. K. W. Nanoplasmonics: Classical down to the Nanometer Scale. *Nano Lett.* **2012**, *12*, 1683–1689.
32. Wu, L.; Duan, H.; Bai, P.; Bosman, M.; Yang, J. K. W.; Li, E. Fowler-Nordheim Tunneling Induced Charge Transfer Plasmons between Nearly Touching Nanoparticles. *ACS Nano* **2013**, *7*, 707–716.
33. Tan, S. F.; Wu, L.; Yang, J. K. W.; Bai, P.; Bosman, M.; Nijhuis, C. A. Quantum Plasmon Resonances Controlled by Molecular Tunnel Junctions. *Science* **2014**, *343*, 1496–1499.
34. Liu, L.; Wang, Y.; Fang, Z.; Zhao, K. Plasmon Hybridization Model Generalized to Conductively Bridged Nanoparticle Dimers. *J. Chem. Phys.* **2013**, *139*, 064310.
35. Knight, M. W.; King, N. S.; Liu, L.; Everitt, H. O.; Nordlander, P.; Halas, N. J. Aluminum for Plasmonics. *ACS Nano* **2014**, *8*, 834–840.